Osmotic stabilization prevents cochlear synaptopathy after blast trauma

Jinkyung Kim[a], Anping Xia[a], Nicolas Grillet[a], Brian E. Applegate[b], and John S. Oghalai[c,1]

[a]Department of Otolaryngology-Head and Neck Surgery, Stanford University, Stanford, CA 94305; [b]Department of Biomedical Engineering, Texas A&M University, College Station, TX 77843; and [c]Caruso Department of Otolaryngology-Head and Neck Surgery, University of Southern California, Los Angeles, CA 90033

Edited by Dan H. Sanes, New York University, New York, NY, and accepted by Editorial Board Member Nancy Y. Ip April 4, 2018 (received for review November 20, 2017)

Traumatic noise causes hearing loss by damaging sensory hair cells and their auditory synapses. There are no treatments. Here, we investigated mice exposed to a blast wave approximating a roadside bomb. In vivo cochlear imaging revealed an increase in the volume of endolymph, the fluid within scala media, termed endolymphatic hydrops. Endolymphatic hydrops, hair cell loss, and cochlear synaptopathy were initiated by trauma to the mechanosensitive hair cell stereocilia and were K^+-dependent. Increasing the osmolality of the adjacent perilymph treated endolymphatic hydrops and prevented synaptopathy, but did not prevent hair cell loss. Conversely, inducing endolymphatic hydrops in control mice by lowering perilymph osmolality caused cochlear synaptopathy that was glutamate-dependent, but did not cause hair cell loss. Thus, endolymphatic hydrops is a surrogate marker for synaptic bouton swelling after hair cells release excitotoxic levels of glutamate. Because osmotic stabilization prevents neural damage, it is a potential treatment to reduce hearing loss after noise exposure.

endolymphatic hydrops | in vivo imaging | cochlea | optical coherence tomography | hearing loss

About 15% of Americans have hearing loss due to noise exposure (1). The classic explanation is trauma to the cochlear hair cells. Hair cell stereociliary bundles transduce the mechanical energy of sound into electro-chemical signals, and because they are highly mechanosensitive they are easily damaged by loud sounds. Through a variety of pathways (2, 3), hair cell death occurs, causing permanent hearing loss evidenced by elevated auditory thresholds. An additional mechanism of noise-induced hearing loss is cochlear synaptopathy. Excess release of glutamate, the hair cell afferent neurotransmitter, occurs primarily through hair cell overstimulation or secondarily after extracellular ATP released from other traumatized cells activate Ca^{+2} channels (4, 5). This results in the toxic entry of ions and water into synaptic boutons (6–8), which damages the dendrite and produces loss of synaptic ribbons in residual hair cells (9–11). Loss of auditory neurons does not necessarily elevate the threshold of hearing, but instead affects neural encoding at higher sound intensities, and so it has been called "hidden" hearing loss (12). There are no effective medical treatments to prevent hearing loss via either mechanism after traumatic noise exposure.

Previously, we exposed mice to a blast wave approximating that of a roadside bomb (13). While hair cell loss occurred only in the cochlear base, there was loss of synaptic ribbons and auditory neurons throughout the cochlea. These different patterns of damage suggest that the causes of hair cell and neuronal trauma are different. The pattern of basal hair cell loss is well established, and is due to the increased force applied to their stereociliary bundles and their increased metabolic vulnerability (3, 14). There is no obvious explanation, however, for why the pattern of neuronal damage did not match that of the hair cells.

We hypothesized that disruption of intracochlear fluid homeostasis may play a role (Fig. 1 *A* and *B*). Scala vestibuli and scala tympani contain perilymph, which has high $[Na^+]$ and low $[K^+]$. In contrast, scala media contains endolymph, which has high $[K^+]$ and low $[Na^+]$. Reissner's membrane and the organ of Corti separate the three scalae. Endolymph has constant ionic current flow (15), with K^+ continuously secreted into it by the stria vascularis along the cochlear lateral wall and removed from it through hair cell stereociliary transduction channels and other pathways (16, 17). Therefore, we considered it possible that damage of basal hair cells may alter cochlear fluid homeostasis and produce widespread neural damage.

Results

Blast Exposure Produces Endolymphatic Hydrops. We delivered a single blast wave to an anesthetized adult mouse and then serially imaged the cochlear apical turn in vivo using optical coherence tomography (OCT) (18–20) (Fig. 1 *C* and *D* and Movie S1). All three scalae—Reissner's membrane, the basilar membrane (BM), and the tectorial membrane (TM)—could be resolved. During the first 3 h after the blast, there was progressive bulging of Reissner's membrane, consistent with an increase in endolymph volume, termed endolymphatic hydrops (21) (Fig. 1*E* and Movie S2). Nine hours after the blast, the position of Reissner's membrane began to normalize (Movie S3). By 1 d after the blast, Reissner's membrane returned to a normal position, where it remained throughout the 7-d period we studied (Fig. 1 *F*–*H*).

In contrast, unexposed control mice demonstrated no changes in the position of Reissner's membrane (Fig. 1*I*), indicating that the imaging procedure does not cause endolymphatic hydrops. Following death, Reissner's membrane progressively shifted

Significance

Trauma due to roadside bombs is an unfortunate consequence of modern warfare and terrorist attacks. Hearing loss often occurs because the cochlea is the body's most sensitive pressure transducer. Here, we used in vivo imaging of the mouse cochlea using optical coherence tomography to show that increased endolymph volume correlates with damage to the auditory synapse. Reducing endolymph volume by increasing perilymph tonicity treated the synaptic loss. Therefore, this study identifies a treatment for noise-induced hearing loss. Furthermore, it suggests that this treatment may help patients with Meniere's disease, a disabling syndrome of vertigo and hearing loss due to increased endolymph volume.

Author contributions: J.K., A.X., B.E.A., and J.S.O. designed research; J.K., A.X., and N.G. performed research; J.K., A.X., N.G., and J.S.O. analyzed data; J.K., B.E.A., and J.S.O. wrote the paper; and J.S.O. supervised the entire project.

The authors declare no conflict of interest.

This article is a PNAS Direct Submission. D.H.S. is a guest editor invited by the Editorial Board.

[1]To whom correspondence should be addressed. Email: oghalai@usc.edu.

This article contains supporting information online at www.pnas.org/lookup/suppl/doi:10.1073/pnas.1720121115/-/DCSupplemental.

Published online May 7, 2018.

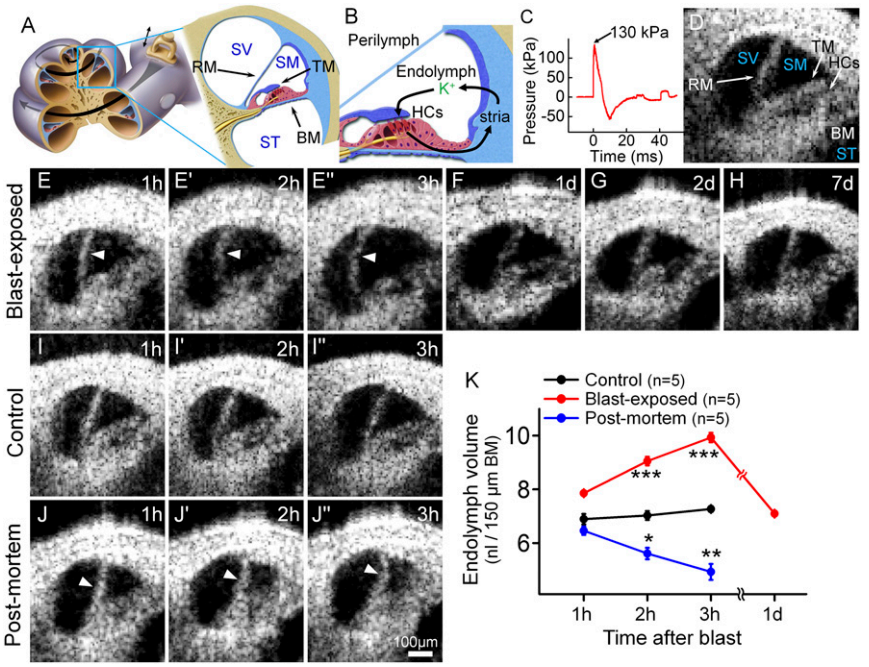

Fig. 1. Blast exposure produces transient endolymphatic hydrops. (*A*) Illustration of the mouse cochlea. The apical turn we studied is expanded. BM, basilar membrane; RM, Reissner's membrane; SM, scala media; ST, scala tympani; SV, scala vestibuli; TM, tectorial membrane. (*B*) Simplified schematic of K^+ flow within the cochlea. K^+ is secreted into endolymph by the stria vascularis (*stria*), taken up by transduction currents through hair cell (HCs) stereociliary bundles, and then passed back to the stria via gap junctions in supporting cells. (*C*) The blast wave pressure monitored by a sensor positioned just below the mouse. (*D*) Cross-sectional OCT image of the mouse cochlea. (*E*) Endolymphatic hydrops (arrowheads) progressively developed within the first 3 h after blast exposure. Images are from one representative mouse. (*F–H*) OCT images from different representative mice 1, 2, and 7 d after blast exposure showed normal endolymph volume. (*I*) OCT images from a representative live control mouse over 3 h demonstrated normal endolymph volume. (*J*) OCT images from an unexposed control mouse followed for 3 h after killing demonstrated progressive reductions of endolymph volume (arrowheads). (*K*) Scala media volume over time in blast-exposed mice, living control mice, and unexposed control mice postmortem. $*P < 0.05$, $**P < 0.01$, $***P < 0.001$.

inward (Fig. 1*J*), consistent with reduced endolymph secretion by the stria vascularis postmortem (16, 22). We then quantified endolymph volume within scala media and perilymph volume within scala vestibuli (Fig. 1*K* and Fig. S1). This confirmed that these fluid volumes changed dynamically and in opposite directions.

Loss of Outer Hair Cells After Blast Exposure. To assess for permanent injury, we counted hair cells 7 d after the blast. This confirmed the pattern of basal outer hair cell (OHC) loss with no loss of inner hair cells (IHCs) (Fig. 2 *A* and *B*). We then immunolabeled hair cells for myosin VIIa within the basal cochlear epithelium at various time points during the first 24 h (Fig. 2 *C–F*). Mice killed immediately following blast exposure exhibited no morphological evidence of OHC damage. Mice killed after 1 h demonstrated clumping of myosin VIIa within some OHCs, consistent with cellular degradation. This was more prevalent 3 h after blast exposure. Mice killed after 1 d demonstrated no clumping but did have substantial OHC loss. Thus, the number of OHCs that were missing or damaged increased over the 7 d following blast exposure (Fig. 2*G*).

To characterize DNA fragmentation, a hallmark of apoptosis, we performed the TUNEL assay on the basal cochlear epithelium (Fig. 2 *H–L*). The percentages of $TUNEL^+$ OHCs immediately following the blast were nearly identical to the percentages of OHC loss 7 d after the blast (Fig. 2*B*). This indicates that OHC fate was determined by the initial trauma of the blast, not from secondary factors arising later, such as endolymphatic hydrops.

Because the stereociliary bundle is the most sensitive mechanical component of the cochlea, OHC death may be initiated by stereociliary trauma. Scanning electron microscopy of basal OHCs from unexposed control mice ($n = 3$) exhibited normal bundle organization (Fig. 2*M*). The stereocilia within each bundle were evenly spaced and had an equal height within each row. In contrast, mice killed immediately after blast exposure ($n = 3$) had distorted bundle morphology (Fig. 2*N*). Many stereocilia were fused together or bent. Some regions of the bundles were missing stereocilia. Thus, blast exposure appeared to cause immediate stereociliary damage.

Cochlear Synaptopathy After Blast Exposure. To assess for hair cell–auditory neuron synapse damage, we counted the number of synaptic ribbons per residual OHC and IHC 7 d after blast exposure by immunolabeling for CtBP2, a marker for the presynaptic hair cell ribbon (Fig. 2 *O* and *P*). Throughout the cochlea, there were significant reductions in the number of synaptic ribbons per OHC and IHC (Fig. 2 *Q* and *R*), although we could not study the IHCs in the base because their vertical orientation made it hard to consistently acquire the high-quality images necessary to count synaptic ribbons.

There was no TUNEL labeling of spiral ganglion neurons within cross-sections of cochleae harvested immediately and 1 d after blast exposure, nor in unexposed controls ($n = 4$ for each case) (Fig. S2). Thus, although hair cell fate is set immediately following the blast, spiral ganglion neuron fate is not.

Perilymph Does Not Mix with Endolymph After Blast Exposure. OHCs that die could create holes in the epithelium. If the surrounding cells take longer to deform and seal the defect than it takes for the OHCs to be evacuated, perilymph might enter scala media and produce endolymphatic hydrops (23–25). To test this hypothesis, we rapidly perfused gold nanoparticles throughout the perilymph. We performed serial imaging to localize the nanoparticles during the perfusion and for 30 min afterward. Because

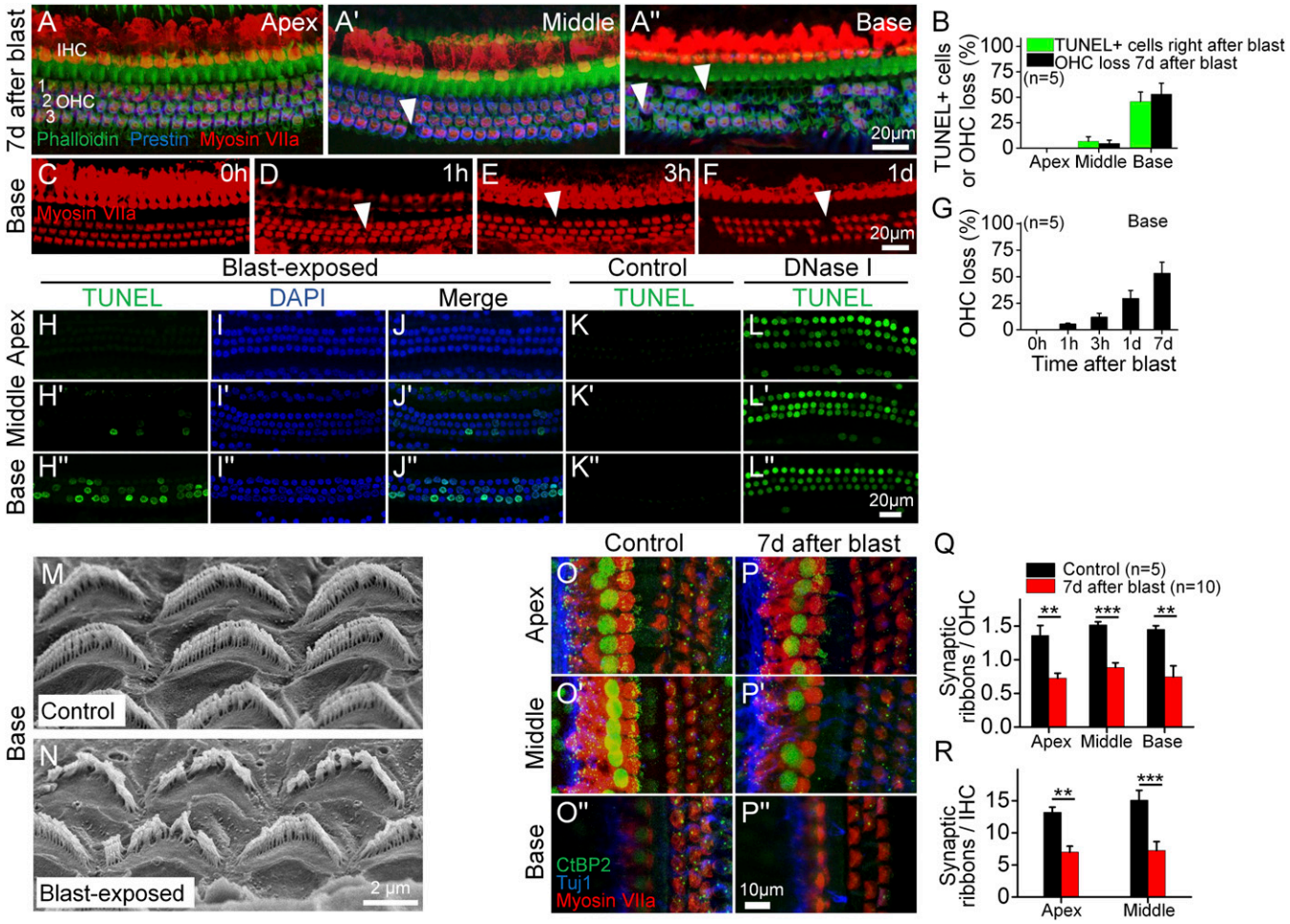

Fig. 2. Blast exposure causes stereociliary trauma, hair cell loss, and cochlear synaptopathy. (*A*) The cochlear epithelium 7 d after blast exposure. Immunolabeling was done to visualize all hair cells (myosin VIIa) and outer hair cells (OHCs) (Prestin). Representative locations of missing hair cells are shown (arrowheads). (*B*) Quantification of OHC loss 7 d after blast exposure and TUNEL$^+$ cells right after blast exposure in the apical, middle, and basal regions. (*C–F*) Representative examples of the cochlear epithelium from the basal region immediately following blast exposure (0 h) and at several time points afterward. (*G*) Progressive OHC loss in the cochlear base. (*H–L*) The cochlear epithelium harvested from a mouse immediately following blast exposure (*H–J*), from an unexposed mouse (negative control, *K*), and from an unexposed mouse in which DNase I was applied to the cochlea (positive control, *L*). The TUNEL assay labels cells with fragmented DNA, which detects apoptotic programmed cell death. (*M* and *N*) Scanning electron microscopic images of OHC stereociliary bundles in representative control and blast-exposed mice. (*O* and *P*) The cochlear epithelium 7 d after blast exposure. Immunolabeling was done to visualize synaptic ribbons in hair cells (CtBP2), hair cells (myosin VIIa), and auditory neurons (Tuj1). (*Q* and *R*) Quantification of synaptic ribbons per OHC and IHC in control and blast-exposed mice. $^{**}P < 0.01$, $^{***}P < 0.001$.

both endolymphatic hydrops and OHC degeneration were obvious 3 h after the blast, we chose this time point to start the experiment.

The perfused gold nanoparticles filled both scala vestibuli and scala tympani, whereas scala media remained clear in blast-exposed and control mice (Fig. 3 and Movies S4 and S5). To quantify this, both cohorts demonstrated large increases in signal intensity within scala vestibuli. However, no significant changes were found within scala media for either cohort. These data argue that posttraumatic endolymphatic hydrops does not result from defects in the endolymph–perilymph barrier larger than 50 nm, consistent with the concept that swelling of the Deiters cell phalangeal processes seal defects in the reticular lamina when OHCs die (23).

Stereociliary Trauma Is the First Step in the Development of Blast-Induced Cochlear Trauma. Next, we examined *Tecta*$^{C1509G/C1509G}$ mice, in which the TM does not deflect the OHC stereocilia because it is detached from the epithelium (26). Previously, we found that 2 h of noise exposure did not cause hair cell loss in this mouse strain, whereas it did in controls (14). Similarly, we found no hair cell loss 7 d after blast exposure (Fig. S3). Furthermore, there was no change in endolymph volume after blast exposure (Fig. 4 *A–C*). These data indicate that blast-induced stereociliary trauma occurs because the bundle is sheared by the TM, and that, in our animal model, this trauma initiates the damage cascade that leads to hair cell loss and endolymphatic hydrops.

Osmotic Gradients Modulate Endolymph Volume. Endolymphatic [K^+] depends on K^+ entry and exit rates; this may affect the osmotic load and thereby modulate endolymph volume (27–30). For example, death inhibits K^+ secretion (22), which correlates with reduced endolymph volume. Furthermore, stereociliary damage after traumatic exposure impairs transduction, reduces K^+ bias currents (31), and correlates with increased endolymph volume. Compared with unexposed controls, unexposed *Tecta*$^{C1509G/C1509G}$ mice had distention of Reissner's membrane and increased endolymph volume ($P = 0.002$) (compare Figs. 1*K* and 4*C*). This is consistent with reduced K^+ bias currents through transduction channels because of the lack of a static bundle deflection in Tecta mutant mice (26, 32, 33) (Fig. 4*D*).

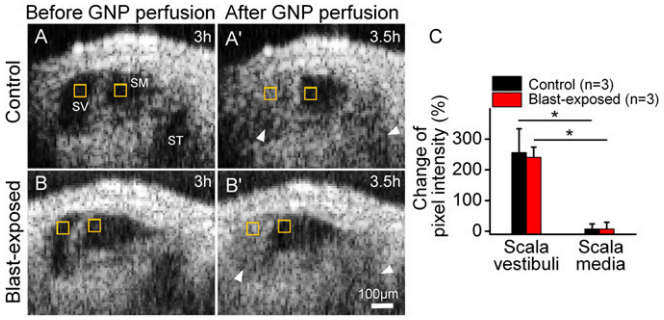

Fig. 3. Perilymph and endolymph do not mix after blast exposure. Gold nanoparticles (GNP) were perfused through the perilymph. (*A*) OCT images of a representative unexposed control mouse 3 h after performing the surgical exposure (*A*) and 30 min after GNP perfusion (*A′*). (*B*) OCT images in a representative mouse 3 h after blast exposure (*B*) and 30 min after GNP perfusion (*B′*). In both conditions, GNP could be detected within the perilymphatic chambers (SV and ST, arrowheads) but not within endolymphatic (SM). (*C*) Measurement of the pixel intensity of discrete regions within SV and SM (yellow boxes) before and 30 min after the perfusion. The percent change in pixel intensity was calculated by normalizing the change in pixel intensity to the pixel intensity before perfusion. $*P < 0.05$.

To better define the role of K^+ in modulating endolymph volume, we studied *Tyr*-DT-A mice, in which ablation of stria intermediate cells abolishes K^+ secretion (34) (Fig. 4 *E–H*). Unexposed *Tyr*-DT-A mice demonstrated an inward deflection of Reissner's membrane and reduced endolymph volume compared with controls ($P = 0.007$), which did not change after blast. As confirmation, we injected CBA mice just before blast exposure with furosemide to inhibit the strial Na-K-Cl cotransporter NKCC2 that secretes K^+. Endolymph volume remained stable after blast exposure in these mice (Fig. 4 *I–L*). Together, these data argue that K^+ is required to develop blast-induced endolymphatic hydrops.

We directly tested whether changing perilymph tonicity affects endolymph volume by perfusing artificial perilymph in control CBA mice over 3 min (Fig. 5 *A–C*). Consistent with this prediction, Reissner's membrane bowed outward with hypotonic, remained in a normal position with normotonic, and bowed inward with hypertonic perilymph. Perilymphatic perfusion requires opening the cochlea, risking hearing loss, and so this technique is not used clinically for inner ear drug delivery. However, round window application is safe (35–37), and we found that this clinical technique also works with osmotic challenge (Fig. 5 *D–I*). Reissner's membrane shifted in accordance with the applied tonicity and the effect did not depend upon the solute used. However, osmotic gradients >300 mM were required to see displacements in Reissner's membrane with round window application, whereas gradients of only 10 mM were needed with perilymphatic perfusion. Regardless, these data demonstrate that osmotic gradients between endolymph and perilymph modulate endolymph volume and these effects are not ion-specific.

Hypertonic Challenge Reverses Endolymphatic Hydrops and Rescues Synaptic Ribbon Loss. We then tested whether osmotic challenge modulates cochlear blast trauma by applying artificial perilymph to the round window 3 h after blast exposure. Normotonic perilymph had no effect, whereas hypertonic perilymph reversed the posttraumatic endolymphatic hydrops (Fig. 5 *J–L*).

Because OHC fate was set immediately by the blast trauma, we did not expect that treating endolymphatic hydrops would rescue hair cells. However, treating endolymphatic hydrops may alter cochlear synaptopathy. For example, patients with Meniere's disease, who have endolymphatic hydrops, have afferent neuron loss beyond that predicted by damage to hair cells (38, 39). This finding has been replicated in animal models of endolymphatic hydrops (40, 41).

We therefore performed a blinded, randomized, prospective study comparing normotonic versus hypertonic artificial perilymph treatment of blast-exposed CBA mice. Thirty minutes after blast exposure, the treatment solution was applied to the left round window. The untreated right ear was a control. Another control group consisted of age-matched mice that were not blast-exposed. Two months later, we counted OHCs and synaptic ribbons (Fig. 5 *M–O*).

While unexposed control mice had no OHC loss, untreated ears from blast-exposed mice had substantial loss of OHCs in the base, scattered loss in the middle, and no loss in the apex. Hair cell counts were no different between the untreated ears and those treated with normotonic or hypertonic artificial perilymph (Fig. 5*P*). Compared with unexposed control mice, there were 36–51% reductions in the number of synaptic ribbons per OHC and IHC in untreated ears and in ears treated with normotonic artificial perilymph (Fig. 5 *Q* and *R*). However, treatment with hypertonic artificial perilymph prevented 45–64% of this loss. Thus, hypertonic treatment of posttraumatic endolymphatic hydrops preserved roughly half the synaptic ribbons that would have been lost without treatment, but had no impact on OHC loss.

As confirmation, we performed a second blinded, randomized, prospective study, but instead tested normotonic and hypertonic NaCl solutions rather than artificial perilymph. Hair cell and synaptic ribbon counts 7 d after the blast exposure were consistent with those of the first trial (Fig. S4).

Auditory Physiology After Blast Exposure. To assess whether hypertonic treatment preserves cochlear function after blast trauma, we measured auditory brainstem responses (ABRs) and distortion product otoacoustic emissions (DPOAEs) during the first trial (Fig. S5 *A–J*). ABR thresholds partially recovered and stabilized 1 mo after the blast exposure, whereas DPOAE thresholds demonstrated no meaningful recovery. There were no differences in average threshold recovery between the cohorts. We also measured the peak-to-peak of ABR wave 1 for all stimulus intensities 2 mo after the blast exposure (Fig. S6 *A–C*); however, there were no differences between the three cohorts. We then further analyzed this data by normalizing the peak-to-peak value at a suprathreshold levels [70-dB sound-pressure level (SPL)] to the preblast values (Fig. S6*D*), but again there were no differences. This surprised us because this measurement has been shown to correlate with cochlear synaptopathy, even with OHC loss (42).

To understand this result, we measured mechanical responses of the BMs and TMs to sound. Control mice demonstrated compressive nonlinearities consistent with cochlear amplification (20, 43) with ~100-nm peak vibratory responses (Fig. 6 *A–C*) ($n = 3$). However, blast-exposed mice demonstrated significant variability (Fig. S5 *K–P*). Some mice responded with compressive nonlinearities, some had passive responses, indicating no cochlear amplification, and some demonstrated no vibration at all. A consistent finding, however, was that none of the blast-exposed mice had peak vibratory responses larger than 10 nm. These findings argue that the blast exposure caused variable degrees of cochlear, and possibly also middle ear, damage (13). Therefore, improvements in ABR wave I responses that theoretically should result with hypertonic treatment are masked by the large variability in damage patterns.

How Does Endolymphatic Hydrops Adversely Affect the Cochlea? To remove these confounding effects of variability in the trauma, we studied mice exposed to band-pass–filtered white noise. Similar noise protocols produce minimal or no OHC loss in the base and a reduction of synaptic ribbons in residual hair cells throughout the cochlea (11, 14). In contrast to control mice that had sharp tuning and large gains of cochlear amplification (BM: 62.3 ± 0.6 dB, TM: 65.3 ± 0.5 dB, $n = 3$, 11 kHz), mice exposed to noise developed endolymphatic hydrops and vibratory responses with broad tuning and little gain (Fig. 6 *D–F*) (BM: 9.2 ± 1.2 dB, TM:

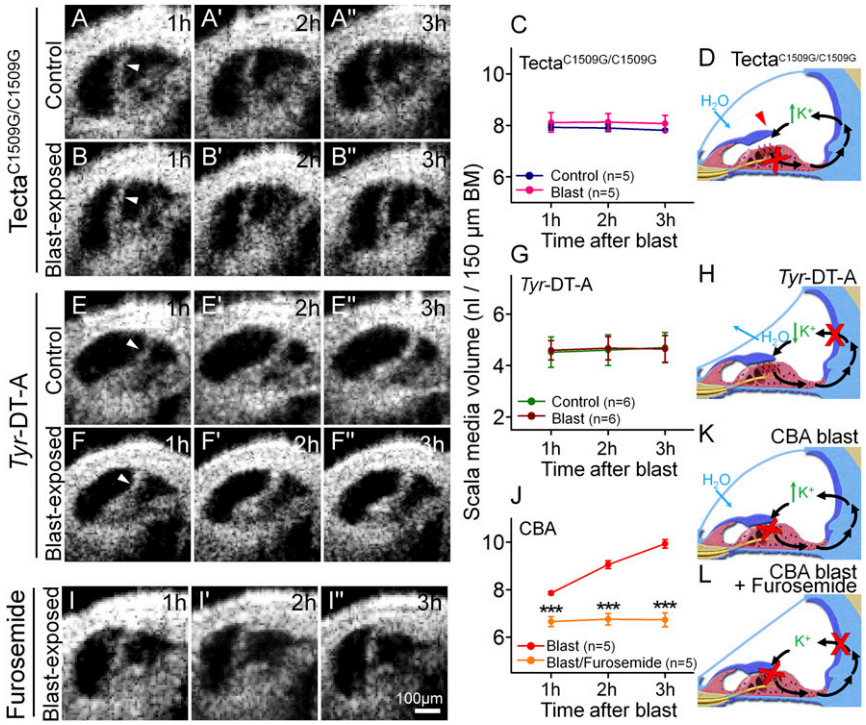

Fig. 4. Stereociliary trauma and endolymphatic K^+ are necessary for the development of endolymphatic hydrops after blast exposure. (*A*) A representative unexposed *Tecta*$^{C1509G/C1509G}$ mouse demonstrates a stable, but increased, volume of endolymph. (*B*) A representative *Tecta*$^{C1509G/C1509G}$ mouse after blast exposure. (*C*) Endolymph volume was higher than normal, yet unchanged by blast-exposure in *Tecta*$^{C1509G/C1509G}$ mice. (*D*) Postulated mechanism of endolymph volume dysregulation in *Tecta*$^{C1509G/C1509G}$ mice. The TM is elevated off the epithelium and so does not cause any static displacement of the OHC stereociliary bundles. Thus, K^+ bias currents through transduction channels (red X) are reduced, increasing endolymph [K^+]. H_2O enters endolymph because of the increased osmotic load. (*E*) A representative unexposed *Tyr*-DT-A mouse demonstrates a stable, but decreased, volume of endolymph. (*F*) A representative *Tyr*-DT-A mouse after blast exposure. (*G*) Endolymph volume in *Tyr*-DT-A mice was lower than normal, yet unchanged, by blast exposure. (*H*) Postulated mechanism of endolymph volume dysregulation in *Tyr*-DT-A mice. K^+ secretion from the stria vascularis is blocked (red X), reducing endolymph [K^+]. H_2O leaves endolymph because the osmotic load is now higher in perilymph. (*I*) A representative CBA mouse that was dosed with furosemide and then exposed to a blast. (*J*) Endolymph volume did not increase after blast exposure in mice pretreated with furosemide. (*K*) Postulated mechanism of endolymph volume dysregulation in CBA mice after blast exposure. Damaged stereocilia and OHC loss (red X) reduce K^+ bias currents through transduction channels (red X), increasing endolymph [K^+] and drawing in H_2O. (*L*) With furosemide treatment, K^+ secretion by the stria is also blocked, so endolymphatic [K^+] is expected to remain stable. ***$P < 0.001$.

17.9 ± 2.7, $P < 0.001$ for both comparisons, $n = 3$, 5 kHz). Thus, noise trauma clearly impacted OHC function but the role of endolymphatic hydrops in causing this effect remained unclear.

Next, we induced endolymphatic hydrops in mice without noise trauma by applying a hypotonic challenge to the round window for 5.5 h. These mice had vibratory response curves and gains similar to controls (Fig. 6 *G–I*) (BM: 59.3 ± 1.0 dB, TM: 60.3 ± 2.5 dB, $n = 4$, 11 kHz, $P = 0.06$ and 0.12). Therefore, isolated endolymphatic hydrops (i.e., not associated with mechanical trauma of stereociliary bundles) does not alter OHC based cochlear amplification. However, synaptic ribbon counts were reduced after the hypotonic challenge to a level similar to that found after blast exposure, even though there was no loss of OHCs ($n = 4$) (Fig. 6 *J–L*). Thus, endolymphatic hydrops in isolation causes cochlear synaptopathy.

Finally, we studied both the pre- and postsynaptic sides of the IHC synapse after perilymphatic perfusion of either normotonic or hypotonic artificial perilymph over 1 h by also immunolabeling postsynaptic densities with Homer (44) (Fig. 6 *M–P*). Mice perfused with hypotonic perilymph had lower CtBP2 and Homer puncta counts than those perfused with normotonic perilymph. However, blocking the AMPA glutamate receptor with CNQX preserved both CtBP2 and Homer puncta counts. The rates of CtBP2/Homer puncta colocalization were reduced with hypotonic perfusion but preserved with the addition of CNQX (Fig. 6*Q*). Thus, hypotonic challenge induces glutamate secretion that not only damages both sides of synaptic cleft but also disrupts pre- and postsynaptic pairing.

Discussion

Blast-induced hearing loss is an increasingly common cause of disability because improvised explosive devices often injure without killing. Our data reveal several fundamental mechanisms that underlie blast-induced sensorineural hearing loss (Fig. 6*R*). The initiating step is trauma to the OHC stereociliary bundle. The fate of the traumatized OHC is set immediately. However, cochlear synaptopathy has a delayed-onset involving several steps. First, endolymphatic hydrops occurs, likely because K^+ is not removed fast enough from the endolymph after the stereociliary trauma. Hair cells then release excess glutamate, which may occur because the posttraumatic endolymphatic hydrops overstimulates them or because nearby damaged cells release ATP that create calcium waves across the epithelium (5, 45). The excitotoxicity of excess glutamate causes ion and H_2O entry into synaptic boutons, and this swelling is associated with either temporary or permanent damage (6–8). Finally, the loss of the bouton leads to loss of synaptic ribbons inside the hair cell. Thus, the most significant finding of this study is that osmotically stabilizing the cochlear fluids after the blast exposure prevents cochlear synaptopathy, even though hair cell fate remains unchanged.

We could perform this study because modern optical techniques permitted in vivo cochlear imaging. Previously, endolymph volume has been assessed indirectly with electrophysiological

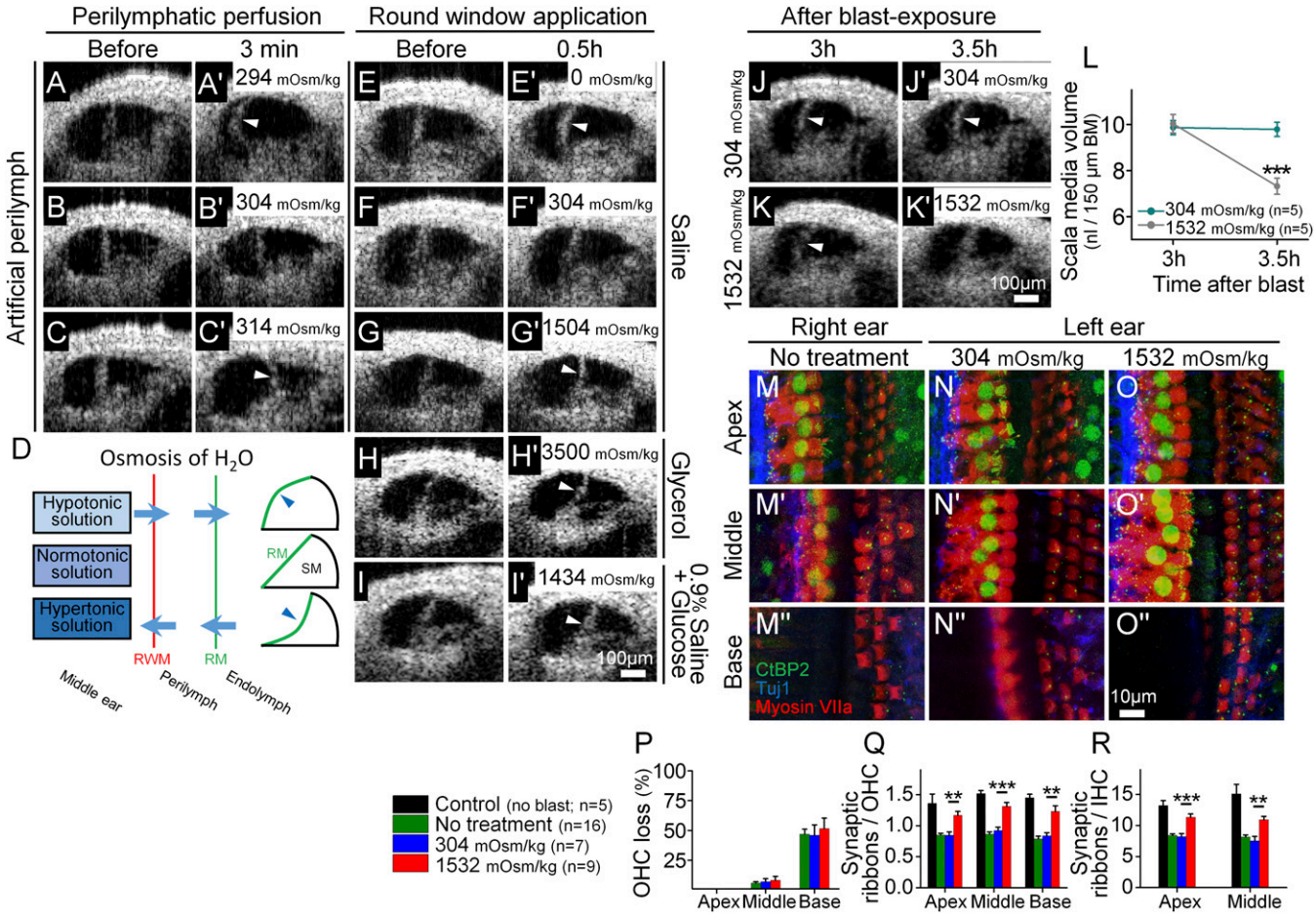

Fig. 5. Osmotic treatment of endolymphatic hydrops partially rescues synaptic ribbon loss after blast exposure. (*A–C*) Perilymph osmolality modulates endolymph volume. Perfusion of hypotonic (*A*), normotonic (*B*), or hypertonic (*C*) artificial perilymph dynamically shifted the position of Reissner's membrane (arrowheads). This occurred rapidly (<3 min). (*D*) Simple model of noninvasive osmotic challenge via the round window membrane (RWM) to alter the volume of endolymph and shift Reissner's membrane (RM). Hypotonic solution applied to the middle ear causes endolymphatic hydrops, whereas hypertonic solution reduces endolymphatic volume. (*E–I*) The application of solutions of varying osmotic loads into the middle ear adjacent to the round window modulates endolymph volume. Representative OCT images were taken before and 30 min after applying the osmotic challenge. Hypotonic challenge (*E*) increased endolymph volume, normotonic saline (*F*) caused no change in endolymph volume, and hypertonic challenges (*G–I*) decreased endolymph volume. (*J* and *K*) Representative mice were treated with normotonic or hypertonic challenge 3 h after blast exposure. Repeat images were taken 30-min later. (*L*) Normotonic artificial perilymph had no impact on posttraumatic endolymphatic hydrops, whereas hypertonic artificial perilymph normalized endolymphatic volume. (*M–O*) The cochlear epithelium from representative mice 2 mo after blast exposure. Mice had either no treatment (*M*), normotonic artificial perilymph application to the middle ear after the blast (*N*), or hypertonic artificial perilymph application to the middle ear after the blast (*O*). Immunolabeling was done to visualize synaptic ribbons in hair cells (CtBP2), hair cells (myosin VIIa), and auditory neurons (Tuj1). (*P–R*) Quantification of OHC loss and synaptic ribbons per OHC and IHC. Hypertonic artificial perilymph reduced the loss of synaptic ribbons but did not affect the degree of OHC loss. $^{**}P < 0.01$, $^{***}P < 0.001$.

parameters (46, 47) or by postmortem histology (48), but neither approach clearly reveals the dynamic nature of endolymph volume. Another strength of this study is that a single blast exposure created the trauma, permitting us to follow the time course of the cochlear response. This is also a weakness, because blast trauma is not necessarily comparable to a lower level of chronic noise exposure like most people experience. Additionally, we did not detect ABR improvements after treatment because the blast caused more than just cochlear synaptopathy. It also caused variable degrees of mechanical damage that affected the traveling wave, as demonstrated by our cochlear vibrometry measures. Therefore, we do not believe that the wave 1 ABR amplitude is a meaningful way to assess for cochlear synaptopathy in this mouse model, where there is significant variability in cochlear mechanics. Nevertheless, both blast and noise exposure produced endolymphatic hydrops. Furthermore, as assessed by immunolabeling, the degree of synaptopathy found after blast exposure was similar to that found with common noise protocols (11, 49).

After loud noise exposure, it is common to experience a sense of aural fullness, which is probably endolymphatic hydrops. Presumably, endolymphatic hydrops resolves as the mechanoelectrical transduction apparatus recovers in surviving OHCs. It is reasonable to assume that the period of endolymphatic hydrops defines the optimal time frame for treatment to minimize long-term sequelae. However, endolymphatic hydrops may simply be a surrogate marker for swelling of the auditory nerve dendrites, and hyperosmotic treatment shrinks both endolymph volume and dendrite volume. In addition, the idea that some dendrites might not be lost, but just temporarily swollen and dysfunctional, is important. Nevertheless, it is clear that permanent cochlear synaptopathy also results (50–52). Osmotically stabilizing the inner ear after noise exposure may offer an important novel therapeutic approach to preserve function. Blockade of damage pathways within the hair cells upstream of synapse loss may also prevent synaptopathy. We show that treatment is efficacious using a middle ear injection technique that is commonly used in the clinic and which could be used on the battlefield.

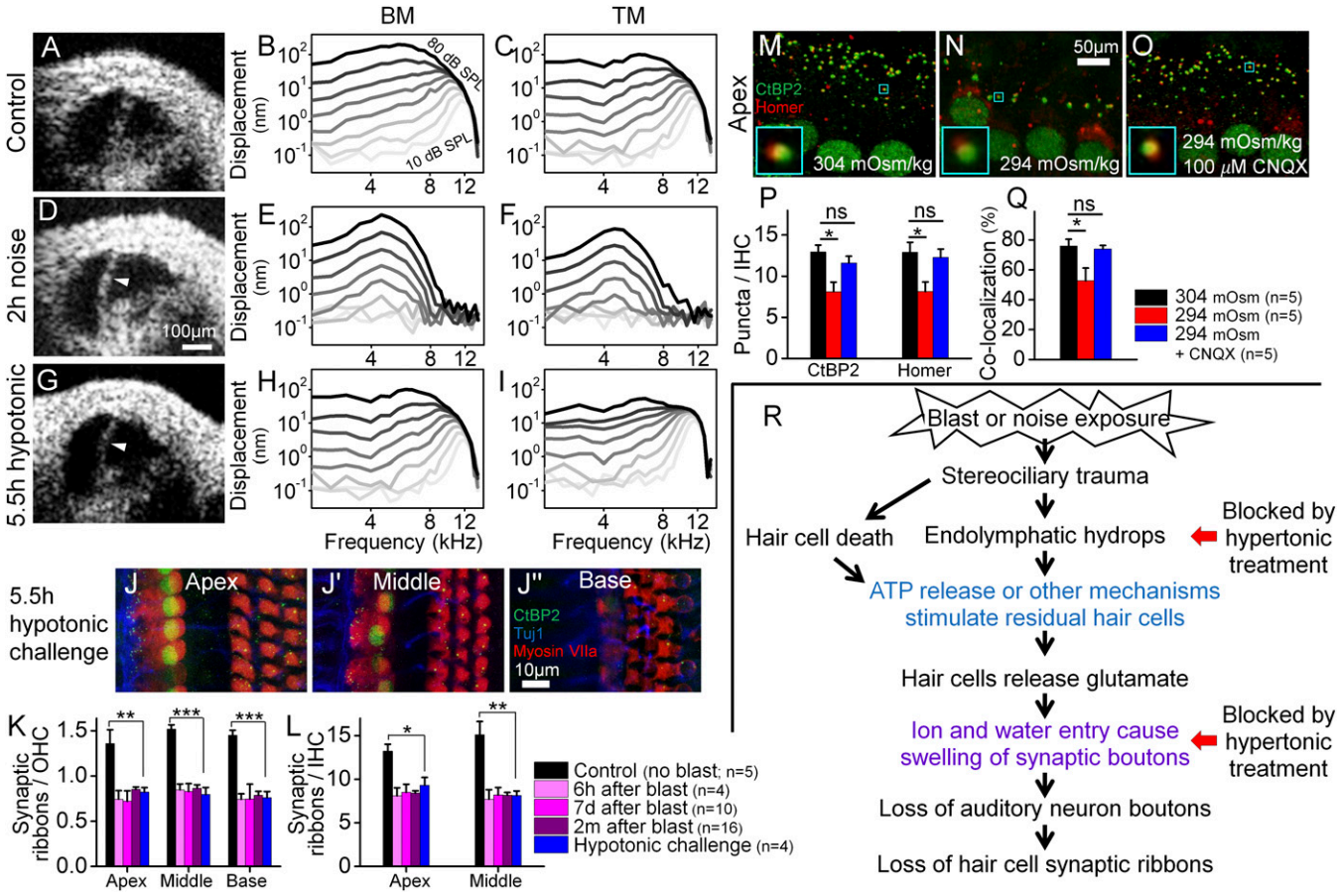

Fig. 6. Endolymphatic hydrops correlates with cochlear synaptopathy, but not loss of hair cells or cochlear amplification. (*A–C*) A representative control mouse with a normal amount of endolymph had normal nonlinear vibratory responses measured from the BM and TM. (*D–F*) A representative mouse with endolymphatic hydrops (arrowhead) induced by 2 h of noise exposure. Vibratory responses were linear, consistent with loss of cochlear amplification. (*G–I*) A representative mouse with endolymphatic hydrops (arrowhead) induced by the application of hypotonic challenge to the middle ear. Vibratory responses for both the BM and TM were normal. (*J*) The cochlear epithelium harvested from a mouse with endolymphatic hydrops induced by hypotonic challenge to the middle ear. (*K* and *L*) Endolymphatic hydrops caused a loss of synaptic ribbons similar to that found after blast exposure. $*P < 0.05$, $**P < 0.01$, $***P < 0.001$. (*M–O*) The cochlear epithelium harvested from representative mice perfused for 1 h with 304 mOsm (*M*), 294 mOsm (*N*), or 294 mOsm + 100 μM CNQX (*O*) artificial perilymph. Immunolabeling was done to visualize presynaptic ribbons in IHCs (CtBP2) and postsynaptic auditory nerve boutons (Homer). Colocalization of the pre- and postsynaptic terminals is shown (*Insets*). (*P*) Hypotonic challenge reduced CtBP2 and Homer counts. Blocking glutamate with CNQX preserved both the pre- and postsynaptic terminals. $*P < 0.05$; ns, not significant. (*Q*) Hypotonic challenge reduced the rate of CtBP2 and Homer colocalization; this effect was also inhibited with CNQX. (*R*) Flowchart detailing our postulated pathophysiological sequence of cochlear damage after blast exposure. The colored text reflects previously published findings [blue (4, 5), violet (6–8)]. Hypertonic challenge blocks both endolymphatic hydrops and swelling of the synaptic boutons (red arrows).

Similarly, this approach may be an alternative treatment for Meniere's disease, in which endolymphatic hydrops causes episodic vertigo, fluctuating hearing loss, and roaring tinnitus (21, 53–56), and dramatically impacts a patient's quality of life.

Materials and Methods

All details are fully described in *SI Materials and Methods*.

In Vivo OCT Imaging and Vibrometry. Under anesthesia, we surgically opened left middle ear bulla to access the apical turn of the cochlea without disturbing the otic capsule bone. The design of our OCT system has been previously reported (20). All studies were carried out according to the protocols that were approved by the Institutional Animal Care and Use Committee at Stanford University (APLAC-23785).

Intracochlear Perilymphatic Perfusion. For "rapid" perfusion (Figs. 3 and 5 *A–C*), the instillation rate was 50 μL/min over 3 min; for "slow" perfusion (Fig. 6 *M–O*), the instillation rate was 8 μL/min over 1 h. Hypotonic artificial perilymph (294 mOsm/kg) was composed of 140 mM NaCl, 2 mM KCl, 2 mM $MgCl_2$, 2 mM $CaCl_2$, and 20 mM Hepes. The osmolality of the perilymph was increased as desired by adding additional Hepes to create normotonic (304 mOsm/kg) and hypertonic (314 mOsm/kg) perilymph.

Application of Solutions to the Round Window Membrane. Normotonic saline (304 mOsm/kg) was composed of 150 mM NaCl and 20 mM Hepes. Hypertonic saline (1,504 mOsm/kg) was composed of 800 mM NaCl and 20 mM Hepes. Normotonic artificial perilymph (304 mOsm/kg) was composed of 140 mM NaCl, 4 mM KCl, 2 mM $MgCl_2$, 2 mM $CaCl_2$, 10 mM Hepes, and 10 mM glucose. Hypertonic artificial perilymph (1,532 mOsm/kg) was created by adding 990 mM glucose to the normotonic artificial perilymph. Hypotonic saline or artificial perilymph was simply distilled water (0 mOsm/kg). Other solutions tested included glycerol (~3,500 mOsm/kg) or 0.9% saline with glucose added to create (1,434 mOsm/kg). For all solutions, the pH was adjusted to 7.4 and the osmolality was verified using a freezing pressure osmometer (Advanced Instruments).

ABR and DPOAE Measurements. ABR potentials were measured with a bioamplifier (Tucker-Davis Technologies) using three needle electrodes positioned in the ventral surface of the tympanic bulla, the vertex of the skull, and the hind leg (57).

DPOAEs were measured by a probe tip microphone in the external auditory canal (57). We used the sound stimuli, two sine wave tones of differing frequencies (F2 = 1.2 × F1, F2: 4 ~ 46 kHz), for eliciting DPOAEs.

Statistical Analysis. All statistical tests not specifically provided in the text are listed in Table S1.

ACKNOWLEDGMENTS. We thank Scott Weldon for the artwork. This project was funded by NIH-National Institute on Deafness and Other Communication Disorders Grants DC014450, DC013774, and DC010363; Department of Defense Grant W81XWH-11-2-0004 (DM090212), and NIH Grant UL1 TR001085.

1. Shargorodsky J, Curhan SG, Curhan GC, Eavey R (2010) Change in prevalence of hearing loss in US adolescents. *JAMA* 304:772–778.
2. Yang C-H, Schrepfer T, Schacht J (2015) Age-related hearing impairment and the triad of acquired hearing loss. *Front Cell Neurosci* 9:276.
3. Furness DN (2015) Molecular basis of hair cell loss. *Cell Tissue Res* 361:387–399.
4. Mammano F, et al. (1999) ATP-induced Ca(2+) release in cochlear outer hair cells: Localization of an inositol triphosphate-gated Ca(2+) store to the base of the sensory hair bundle. *J Neurosci* 19:6918–6929.
5. Piazza V, Ciubotaru CD, Gale JE, Mammano F (2007) Purinergic signalling and intercellular Ca2+ wave propagation in the organ of Corti. *Cell Calcium* 41:77–86.
6. Pujol R, Puel JL (1999) Excitotoxicity, synaptic repair, and functional recovery in the mammalian cochlea: A review of recent findings. *Ann N Y Acad Sci* 884:249–254.
7. Mayer ML, Westbrook GL (1987) Cellular mechanisms underlying excitotoxicity. *Trends Neurosci* 10:59–61.
8. Choi DW, Rothman SM (1990) The role of glutamate neurotoxicity in hypoxic-ischemic neuronal death. *Annu Rev Neurosci* 13:171–182.
9. Moser T, Starr A (2016) Auditory neuropathy—Neural and synaptic mechanisms. *Nat Rev Neurol* 12:135–149.
10. Lin HW, Furman AC, Kujawa SG, Liberman MC (2011) Primary neural degeneration in the guinea pig cochlea after reversible noise-induced threshold shift. *J Assoc Res Otolaryngol* 12:605–616.
11. Kujawa SG, Liberman MC (2009) Adding insult to injury: Cochlear nerve degeneration after "temporary" noise-induced hearing loss. *J Neurosci* 29:14077–14085.
12. Schaette R, McAlpine D (2011) Tinnitus with a normal audiogram: Physiological evidence for hidden hearing loss and computational model. *J Neurosci* 31:13452–13457.
13. Cho S-IIS-I, et al. (2013) Mechanisms of hearing loss after blast injury to the ear. *PLoS One* 8:e67618.
14. Liu CCC, et al. (2011) Biophysical mechanisms underlying outer hair cell loss associated with a shortened tectorial membrane. *J Assoc Res Otolaryngol* 12:577–594.
15. Zidanic M, Brownell WE (1990) Fine structure of the intracochlear potential field. I. The silent current. *Biophys J* 57:1253–1268.
16. Zdebik AA, Wangemann P, Jentsch TJ (2009) Potassium ion movement in the inner ear: Insights from genetic disease and mouse models. *Physiology (Bethesda)* 24: 307–316.
17. Wangemann P (2002) K+ cycling and the endocochlear potential. *Hear Res* 165:1–9.
18. Gao SS, et al. (2014) Vibration of the organ of Corti within the cochlear apex in mice. *J Neurophysiol* 112:1192–1204.
19. Gao SS, et al. (2013) In vivo vibrometry inside the apex of the mouse cochlea using spectral domain optical coherence tomography. *Biomed Opt Express* 4:230–240.
20. Lee HY, et al. (2015) Noninvasive in vivo imaging reveals differences between tectorial membrane and basilar membrane traveling waves in the mouse cochlea. *Proc Natl Acad Sci USA* 112:3128–3133.
21. Schuknecht HF (1993) *Pathology of the Ear* (Lea & Febiger, Philadelphia), 2nd Ed.
22. Patuzzi R (2011) Ion flow in stria vascularis and the production and regulation of cochlear endolymph and the endolymphatic potential. *Hear Res* 277:4–19.
23. Anttonen T, et al. (2014) How to bury the dead: Elimination of apoptotic hair cells from the hearing organ of the mouse. *J Assoc Res Otolaryngol* 15:975–992.
24. Raphael Y, Altschuler RA (1991) Scar formation after drug-induced cochlear insult. *Hear Res* 51:173–183.
25. Kaur T, Hirose K, Rubel EW, Warchol ME (2015) Macrophage recruitment and epithelial repair following hair cell injury in the mouse utricle. *Front Cell Neurosci* 9:150.
26. Xia A, et al. (2010) Deficient forward transduction and enhanced reverse transduction in the alpha tectorin C1509G human hearing loss mutation. *Dis Model Mech* 3: 209–223.
27. Klockhoff I, Lindblom U (1966) Glycerol test in Ménière's disease. *Acta Otolaryngol* 224:224, 449.
28. Eckhard A, et al. (2015) Regulation of the perilymphatic-endolymphatic water shunt in the cochlea by membrane translocation of aquaporin-5. *Pflugers Arch* 467: 2571–2588.
29. Hirt B, et al. (2010) The subcellular distribution of aquaporin 5 in the cochlea reveals a water shunt at the perilymph-endolymph barrier. *Neuroscience* 168:957–970.
30. Konishi T, Hamrick PE, Mori H (1984) Water permeability of the endolymph-perilymph barrier in the guinea pig cochlea. *Hear Res* 15:51–58.
31. Patuzzi R (2002) Non-linear aspects of outer hair cell transduction and the temporary threshold shifts after acoustic trauma. *Audiol Neurotol* 7:17–20.
32. Yuan T, Gao SS, Saggau P, Oghalai JS (2010) Calcium imaging of inner ear hair cells within the cochlear epithelium of mice using two-photon microscopy. *J Biomed Opt* 15:016002.
33. Legan PK, et al. (2000) A targeted deletion in alpha-tectorin reveals that the tectorial membrane is required for the gain and timing of cochlear feedback. *Neuron* 28: 273–285.
34. Kim HJ, et al. (2013) Precise toxigenic ablation of intermediate cells abolishes the "battery" of the cochlear duct. *J Neurosci* 33:14601–14606.
35. Oghalai JS, et al. (2009) Intra-operative monitoring of cochlear function during cochlear implantation. *Cochlear Implants Int* 10:1–18.
36. Cooper NP, Rhode WS (1996) Fast travelling waves, slow travelling waves and their interactions in experimental studies of apical cochlear mechanics. *Aud Neurosci* 2: 289–299.
37. Wenzel GI, et al. (2007) Helper-dependent adenovirus-mediated gene transfer into the adult mouse cochlea. *Otol Neurotol* 28:1100–1108.
38. Nadol JB, Jr (1988) Application of electron microscopy to human otopathology. Ultrastructural findings in neural presbycusis, Menière's disease and Usher's syndrome. *Acta Otolaryngol* 105:411–419.
39. Nadol JB, Jr, Thornton AR (1987) Ultrastructural findings in a case of Menière's disease. *Ann Otol Rhinol Laryngol* 96:449–454.
40. Momin SR, Melki SJ, Alagramam KN, Megerian CA (2010) Spiral ganglion loss outpaces inner hair cell loss in endolymphatic hydrops. *Laryngoscope* 120:159–165.
41. Bixenstine PJ, Maniglia MP, Vasanji A, Alagramam KN, Megerian CA (2008) Spiral ganglion degeneration patterns in endolymphatic hydrops. *Laryngoscope* 118: 1217–1223.
42. Sergeyenko Y, Lall K, Liberman MC, Kujawa SG (2013) Age-related cochlear synaptopathy: An early-onset contributor to auditory functional decline. *J Neurosci* 33: 13686–13694.
43. Lee HY, et al. (2016) Two-dimensional cochlear micromechanics measured in vivo demonstrate radial tuning within the mouse organ of Corti. *J Neurosci* 36:8160–8173.
44. Martinez-Monedero R, et al. (2016) GluA2-containing AMPA receptors distinguish ribbon-associated from ribbonless afferent contacts on rat cochlear hair cells. *eNeuro* 3:ENEURO.0078-16.2016.
45. Chan DK, Rouse SL (2016) Sound-induced intracellular Ca2+ dynamics in the adult hearing cochlea. *PLoS One* 11:e0167850.
46. van Deelen GW, Ruding PR, Veldman JE, Huizing EH, Smoorenburg GF (1987) Electrocochleographic study of experimentally induced endolymphatic hydrops. *Arch Otorhinolaryngol* 244:167–173.
47. Uchida K, Kitahara M, Yazawa Y (1994) Electrocochleography in experimental endolymphatic hydrops. *Acta Otolaryngol Suppl* 510:24–28.
48. Schuknecht HF (1976) Pathophysiology of endolymphatie hydrops. *Arch Otorhinolaryngol* 212:253–262.
49. Liberman LD, Suzuki J, Liberman MC (2015) Dynamics of cochlear synaptopathy after acoustic overexposure. *J Assoc Res Otolaryngol* 16:205–219, and erratum (2015) 16: 221.
50. Plack CJ, Barker D, Prendergast G (2014) Perceptual consequences of "hidden" hearing loss. *Trends Hear* 18:1–11.
51. Bharadwaj HM, Verhulst S, Shaheen L, Liberman MC, Shinn-Cunningham BG (2014) Cochlear neuropathy and the coding of supra-threshold sound. *Front Syst Neurosci* 8:26.
52. Bharadwaj HM, Masud S, Mehraei G, Verhulst S, Shinn-Cunningham BG (2015) Individual differences reveal correlates of hidden hearing deficits. *J Neurosci* 35: 2161–2172.
53. Sajjadi H, Paparella MM (2008) Meniere's disease. *Lancet* 372:406–414.
54. Schuknecht HF (1976) Pathophysiology of endolymphatic hydrops. *Arch Otorhinolaryngol* 212:253–262.
55. Salt AN, Plontke SK (2010) Endolymphatic hydrops: Pathophysiology and experimental models. *Otolaryngol Clin North Am* 43:971–983.
56. Valk WL, et al. (2005) Morphology of the endolymphatic sac in the guinea pig after an acute endolymphatic hydrops. *Hear Res* 202:180–187.
57. Xia A, et al. (2007) Altered traveling wave propagation and reduced endocochlear potential associated with cochlear dysplasia in the BETA2/NeuroD1 null mouse. *J Assoc Res Otolaryngol* 8:447–463.